Soapless Emulsion Polymerization of Methyl Methacrylate. II. Simulation of Polymer Particle Formation

YI-CHENG CHEN, CHIA-FEN LEE, and WEN-YEN CHIU*

Institute of Materials Science and Engineering, National Taiwan University, Taipei, Taiwan

SYNOPSIS

In this work, a generalized mathematical model was developed to estimate the variation of particle concentration during the entire course of soapless emulsion polymerization of methyl methacrylate (MMA). All of the factors, such as oligomeric radical absorption or desorption by polymer particles, coagulation between polymer particles, and the termination effect on the formation mechanism of polymer particles, were considered and included in this model. When appropriate parameters were selected, this model could be successfully used to interpret the experimental behavior of particle concentration during the entire reaction. Under different conditions, the rate of polymerization, the number of radicals in each particle, the instantaneous average molecular weight of polymers, and the rate constant of termination were also calculated. All of them coincided with the experimental results quite well. © 1996 John Wiley & Sons, Inc.

INTRODUCTION

Soapless emulsion polymerization has received more attention in recent decades because it provides advantages for the synthesis of monodisperse latex. In this type of system, polymer particles are stabilized by ionized initiators. Several particle nucleation mechanisms have been proposed for emulsifier free systems, which can be divided into two main categories.

1. Micellar-like nucleation: This was proposed by Van der Hoff,[1] Goodall et al.,[2] Cox et al.,[3] Chen and Piirma,[4] and Vanderhoff.[5] As the oligomeric radicals in the aqueous phase reached critical length, several of them aggregated together to form a micellar-like primary particle and began nucleation.
2. Homogeneous nucleation: This was proposed by Priest,[6] Fitch and Tsai,[7-8] and Hansen and Ugelstad.[9-13] When above the critical chain, each growing oligomeric radical precipitated from the aqueous phase and became a primary particle.

Both the nucleation mechanisms mentioned above could reasonably describe the phenomena of particle nucleation in different soapless emulsion polymerization systems. The former applied if a hydrophobic monomer was used. The latter was more desirable if a hydrophilic monomer was chosen. According to the GPC analysis, Fitch and Tsai found that the maximum degree of polymerization of PMMA oligomers in the aqueous phase was 66. This was accepted as the critical chain length of PMMA oligomers in particle nucleation. Yet Vanderhoff proved that the critical chain length of PS oligomers in the aqueous phase was about four. In homogeneous nucleation, primary particles are unstable because they do not have enough surface charge. These primary particles start to coagulate, and their sizes grow until they have enough charge density on their surfaces to stabilize themselves. Then, the particle concentration in the aqueous phase levels off until the end of the reaction. In this work, a generalized mathematical model was proposed for the homogeneous nucleation of polymer particles to successfully interpret the behavior of particle concentration

* To whom correspondence should be addressed.

Journal of Applied Polymer Science, Vol. 61, 2235–2244 (1996)
 CCC 0021-8995/96/122235-10

during the entire course of soapless emulsion polymerization of MMA.

THEORETICAL TREATMENT

For the soapless emulsion polymerization of MMA with potassium persulfate (KPS) as initiator, the particle generation was certified to follow the mechanism of homogeneous nucleation.[7-8] In the aqueous phase, the KPS initiator decomposed and propagated with the monomer to form oligomers. When the growing oligomers reached their critical chain length, they precipitated from the aqueous phase and formed primary particles; but these primary particles were unstable during the reaction. Coagulation between particles proceeded strenuously at the beginning of the reaction until the polymer particles received enough surface charge. If the nucleation mechanism mentioned above was considered, the following kinetic equations could be derived.

Oligomer Radicals in Aqueous Phase

The rates of formation of oligomer radicals in the aqueous phase[9] could be derived as follows.

For initiator radical,

$$\frac{dR_i}{dt} = \rho_i - k_p \cdot M_w \cdot R_i - k_t \cdot R_{tot} \cdot R_i \quad (1)$$

and

$$\rho_i = 2 \cdot k_d \cdot f \cdot [I] \quad (2)$$

For 1-mer radical,

$$\frac{dR_1}{dt} = k_p \cdot M_w \cdot (R_i - R_1) - k_t \cdot R_{tot} \cdot R_1 - k_{a1} \cdot N_{tot} \cdot R_1 \quad (3)$$

For 2-mer radical,

$$\frac{dR_2}{dt} = k_p \cdot M_w \cdot (R_1 - R_2) - k_t \cdot R_{tot} \cdot R_2 - k_{a2} \cdot N_{tot} \cdot R_2 \quad (4)$$

For j-mer radical,

$$\frac{dR_j}{dt} = k_p \cdot M_w \cdot (R_{j-1} - R_j) - k_t \cdot R_{tot} \cdot R_j - k_{aj} \cdot N_{tot} \cdot R_j \quad (5)$$

where R_i was the concentration of the initiator radical in the aqueous phase, R_j was the concentration of oligomer radical which contained j monomer units, k_p was the propagation rate constant, k_t was the termination rate constant, k_{aj} was the absorption rate constant between j-unit oligomer radicals and polymer particles, M_w was the monomer concentration in the aqueous phase, and N_{tot} was defined as

$$N_{tot} = \sum_{j=0}^{\infty} N_j \quad (6)$$

where N_j was the concentration of polymer particles which contained j radicals. R_{tot} was the total concentration of all radicals in aqueous phase and was expressed as

$$R_{tot} = R_i + \sum_{j=1}^{jcr} R_j \quad (7)$$

In eqs. (3)-(5), the influences of propagation, termination, and absorption of oligomer radicals in the aqueous phase were all included. Summing up eqs. (1)-(5) and assuming that the maximum value of j was jcr (critical chain length), we could obtain

$$\frac{dR_{tot}}{dt} = \rho_i - k_p \cdot M_w \cdot R_{jcr} - k_t \cdot R_{tot}^2 - N_{tot} \cdot \sum_{j=1}^{jcr} k_{aj} \cdot R_j \quad (8)$$

To simplify eq. (8), the average absorption rate constant $\overline{k_a}$ was defined as

$$\overline{k_a} = \left(\sum_{j=1}^{jcr} k_{aj} \cdot R_j \right) \Big/ R_{tot} \quad (9)$$

Substituting eq. (9) into eq. (8), and applying the pseudosteady-state approximation to R_{tot}, it could then be expressed as

$$R_{tot} = \frac{\{[(\overline{k_a} \cdot N_{tot})^2 - 4 \cdot k_t \cdot (k_p \cdot M_w \cdot R_{jcr} - \rho_i)]^{1/2} - \overline{k_a} \cdot N_{tot}\}}{2 \cdot k_t} \quad (10)$$

We found that $\rho_i > k_p \cdot M_w \cdot R_{jcr}$ and $k_t \cdot \rho_i \gg \overline{k_a} \cdot N_{tot}$, and the values of each term were listed in Table I. According to the above assumptions, eq. (10) could be further simplified as

$$R_{\text{tot}} = \left(\frac{\rho_i}{k_t}\right)^{1/2} \tag{11}$$

In this article, eq. (11) was chosen to calculate the total concentration of radicals in the aqueous phase.

Concentration of Polymer Particles

The rate of formation of polymer particles could be determined as follows.[12,14]

$$\frac{dN_0}{dt} = kD \cdot N_1 + \frac{k_t}{V_p \cdot N_A} \cdot N_2 - \overline{k_a} \cdot N_0 \cdot R_{\text{tot}} - k_f \cdot N_0 \cdot N_{\text{tot}} \tag{12}$$

$$\frac{dN_1}{dt} = k_p \cdot M_w \cdot R_{jcr} \cdot (u(t) - u(t - t_0)) - k_f \cdot N_1 \cdot \sum_{j=1}^{n} N_j + kD \cdot \left[\binom{2}{1} \cdot N_2 - \binom{1}{1} \cdot N_1\right] + \frac{k_t}{V_p \cdot N_A} \cdot \binom{3}{2} \cdot N_3 + \overline{k_a} \cdot R_{\text{tot}} \cdot (N_0 - N_1) \tag{13}$$

where $u(t - t_0)$ represented a step function, i.e.,

$$u(t - t_0) = 1 \quad t \geq t_0$$

$$u(t - t_0) = 0 \quad t < t_0$$

$$\frac{dN_2}{dt} = \frac{k_f}{2} \cdot \sum_{j=1}^{2-1} N_j \cdot N_{2-j} - k_f \cdot N_2 \cdot \sum_{j=1}^{n} N_j + \text{kD} \cdot \left[\binom{3}{1} \cdot N_3 - \binom{2}{1} \cdot N_2\right] + \frac{k_t}{V_p \cdot N_A} \left[\binom{4}{2} \cdot N_4 - \binom{2}{2} \cdot N_2\right] + \overline{k_a} \cdot R_{\text{tot}} \cdot (N_1 - N_2) \tag{14}$$

$$\frac{dN_k}{dt} = \frac{k_f}{2} \cdot \sum_{j=1}^{k-1} N_j \cdot N_{k-j} - k_f \cdot N_k \cdot \sum_{j=1}^{n} N_j + kD \cdot \begin{bmatrix} \binom{k+1}{1} \cdot N_{k+1} \\ -\binom{k}{1} \cdot N_k \end{bmatrix} + \frac{k_t}{V_p \cdot N_A} \left[\binom{k+2}{2} \cdot N_{k+2} - \binom{k}{2} \cdot N_k\right] + \overline{k_a} \cdot R_{\text{tot}} \cdot (N_{k-1} - N_k) \quad (k \geq 2) \tag{15}$$

Summing up eqs. (12)–(15), we obtained

$$\frac{dN_{\text{tot}}}{dt} = k_p \cdot M_w \cdot R_{jcr} + kD \cdot \binom{k+1}{1} \cdot N_{k+1} - \overline{k_a} \cdot N_k \cdot R_{\text{tot}} + \frac{k_t}{V_p \cdot N_A} \times \left[\binom{k+2}{2} \cdot N_{k+2} + \binom{k+1}{2} \cdot N_{k+1}\right] - k_f \times \left[\sum_{j=1}^{k} N_j \cdot \sum_{j=1}^{k} N_j + N_0 \cdot \sum_{j=0}^{k} N_j - \sum_{j=1}^{k-1} N_j \cdot \sum_{j=1}^{k-1} N_j\right] \tag{16}$$

where kD was the desorption rate constant, V_p was the volume of one polymer particle, N_A was the Avogadro's number, N_k was the concentration of polymer particles which contained k radicals, and k_f was the average coagulation rate constant between polymer particles.

In the above equations, factors such as propagation and termination effects in the polymer particles, absorption and desorption effects on polymer particle surface, and the coagulation effect between polymer particles were all considered.

According to the Smoluchowski's coagulation equation,[13] k_f could be written as[23]

$$k_f = k_{f0} \cdot \exp\left(\frac{-V_{\text{tot}}}{k \cdot T}\right) \tag{17}$$

where V_{tot} was the total potential energy.[13] Assuming that there was a linear relationship between V_{tot} and reaction time t, i.e., $V_{\text{tot}}(t) = a \cdot t + b$, then k_f could be expressed as

$$k_f = k_{f0} \cdot \exp\left(\frac{-(a \cdot t + b)}{k \cdot T}\right) \tag{18}$$

Combined with k_f in eq. (18), as well as R_{tot} in eq. (11), the concentration of polymer particles, either N_k ($k = 0, 1, 2 \cdots$) or N_{tot}, could be calculated numerically by solving eqs. (12)–(16) simultaneously.

Rate of Polymerization

The rate of polymerization in polymer particles could be expressed as

$$R_p = [M]_0 \cdot \frac{dX}{dt} = k_p \cdot [M]_p \bar{n} \cdot \frac{N_p}{N_A} \tag{19}$$

Table I The Values of the Terms ρ_i, $k_p \cdot M_w \cdot R_{jcr}$, $k_t \cdot \rho_i$, and $\overline{k_a} \cdot N_{tot}$ at Different Experimental Conditions

Experimental Condition	ρ_i	$k_p \cdot M_w \cdot R_{jcr}$	$k_t \cdot \rho_i$	$\overline{k_a} \cdot N_{tot}$
A	2.28×10^{-8}	1.49×10^{-8}	0.55	0.094
B	1.66×10^{-7}	1.83×10^{-8}	0.61	0.094
C	5.69×10^{-8}	1.49×10^{-8}	1.38	0.094

where $[M]_0$ was the total initial amount of monomer charged per unit of aqueous phase, X was the conversion, $[M]_p$ represented the monomer concentration in polymer particles, N_p was the number of polymer particles in the water phase (i.e., $N_p = N_A \cdot N_{tot}$), and $\bar{n}$ expressed the average number of radicals per polymer particle. In eq. (19), R_p was obtained from the conversion-time curve. Furthermore, if the values of k_p, N_p, and $[M]_p$ were known, the variation of $\bar{n}$ with reaction time could be determined.

Average Molecular Weight of Polymers

The relationship between the instantaneous number average molecular weight of polymer and the accumulated number average molecular weight of polymer was described as

$$\overline{Mn} = \frac{X}{\displaystyle\int_0^X \frac{dX}{\overline{Mn}_{inst}(X)}} \tag{20}$$

If the chain transfer reactions were neglected, the instantaneous number average molecular weight $\overline{Mn}_{inst}$ could be calculated approximately by

$$\overline{Mn}_{inst} = M_0 \cdot \frac{R_p}{R_t} = M_0 \cdot \frac{R_p}{\dfrac{k_t}{V_p \cdot N_p} \cdot (\bar{n} \cdot N_p)^2} \tag{21}$$

Combining eqs. (20) and (21) with experimental results of $\overline{Mn}$, the termination rate constant k_t varied with reaction time (or conversion) could be estimated.

RESULTS AND DISCUSSION

All the experimental conditions in the following discussion were listed in Table II.

Monomer Concentration in Polymer Particle $[M]_p$

According to Figure 1, factors such as initiator concentration, agitation speed, and reaction temperature had no significant influence on the magnitudes of monomer concentration in polymer particles. The initial value of $[M]_p$ was kept at 6.0 (mol/L). As the conversion increased over 0.25, $[M]_p$ started to decrease almost in a linear relation with the conversion increase. The following two equations were proposed for the calculation of $[M]_p$ over the entire course of polymerization.

$$\text{I. } X < 0.25, \quad [M]_p = 6.0 \text{ (mol/L)}$$

$$\text{II. } X \geq 0.25, \quad [M]_p = 6.0(1 - X)/(1 - 0.25)(\text{mol/L}) \tag{22}$$

Table II Experimental Conditions

Symbol	Temperature (K)	Initiator Concentration (mol/L-H_2O)	Initial Monomer Concentration (mol/L-H_2O)	Agitation Speed (rpm)
A	343	4.0×10^{-3}	1	300
B	333	4.0×10^{-3}	1	300
C	333	1.0×10^{-2}	1	300
D	333	4.0×10^{-3}	1	500

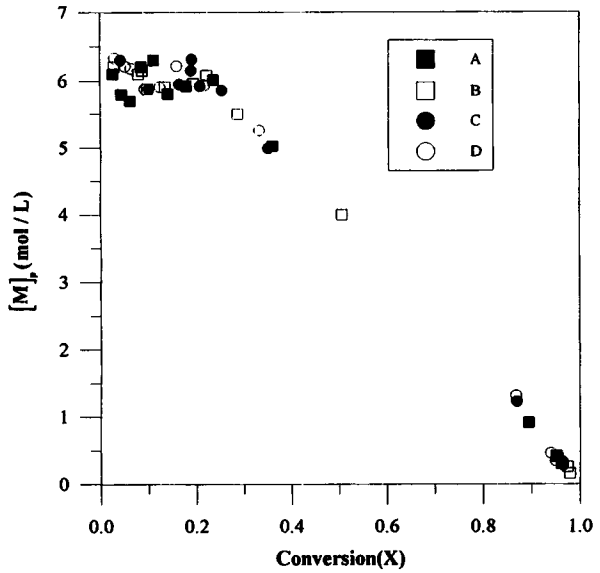

Figure 1 Monomer concentration in polymer particles versus conversion.

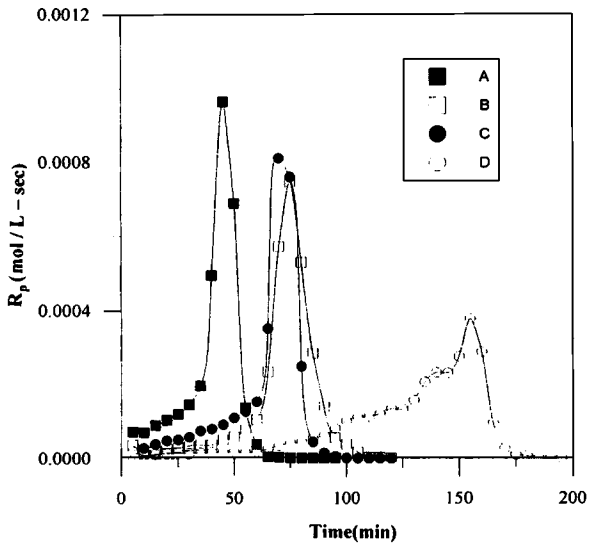

Figure 3 Rate of polymerization versus time.

Rate of Polymerization (R_p)

With eq. (19), the rate of polymerization could be calculated from the experimental curve of conversion versus time (Fig. 2). The result was shown in Figure 3. The dome shape of the curve was a result of the autoacceleration effect. The result showed that higher initiator concentrations accelerated the rate of polymerization (R_p). In addition, the rate of polymerization increased significantly with the temperature increase. But the value of R_p was smaller if a higher agitation speed was chosen.

Concentration of Polymer Particle (N_p)

The value of number average diameter ($\bar{D}$) of polymer particles was obtained by measurement using a transmission electron microscope (TEM). Then we calculated the concentration of polymer particles (N_p).[14] The result was shown in Figure 4.

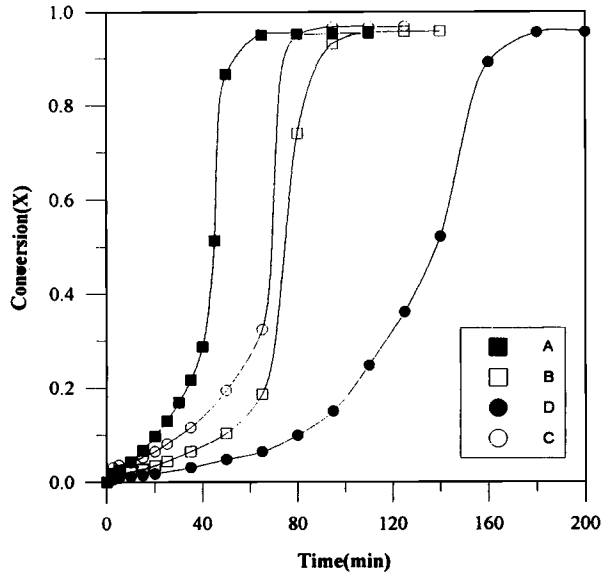

Figure 2 Monomer conversion versus reaction time at different experimental conditions.

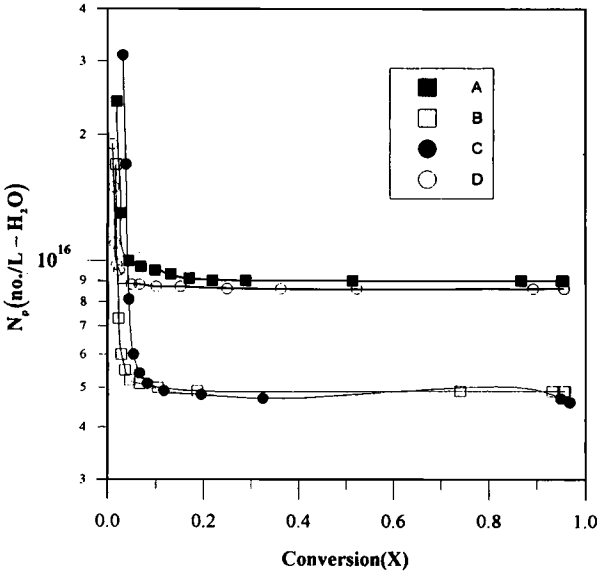

Figure 4 Particle concentration versus conversion at different experimental conditions.

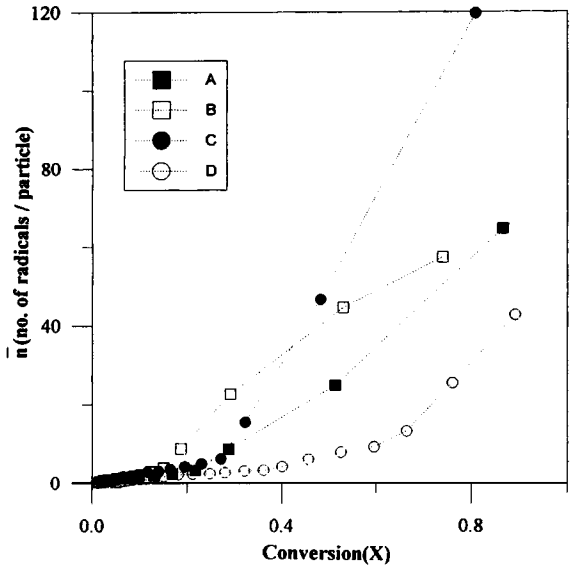

Figure 5 Average number of radicals per polymer particle versus conversion.

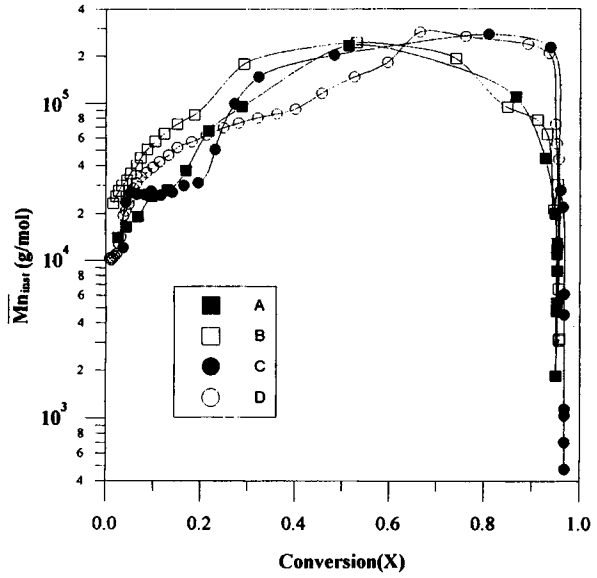

Figure 7 Instantaneous number average molecular weight of polymer versus conversion.

Average Number of Radicals Per Polymer Particle ($\bar{n}$)

Once the calculation of R_p and N_p was completed, as seen in Figure 3 and Figure 4, together with eq. (22) proposed for $[M_p]$, $\bar{n}$ could then be calculated by eq. (19). The result was described in Figure 5. When the conversion was low (less than 15%), $\bar{n}$ was about 0.5, which was in agreement with Smith-Ewart's theory.[19] However, as the conversion got higher, the gel effect gradually became more serious and lessened the probability of polymer free radicals toward termination. Therefore, $\bar{n}$ increased quickly as the conversion was greater. This result also coincided with ESR's study.[15-17] Figure 5 also revealed that the higher the initiator concentration, the larger the final value of $\bar{n}$. The influence of temperatures was that higher temperature lessened the gel effect in polymer particles, so the final value of $\bar{n}$ was lower. As far as the agitation effect was concerned, a higher agitation speed decreased the value of $\bar{n}$. The reason

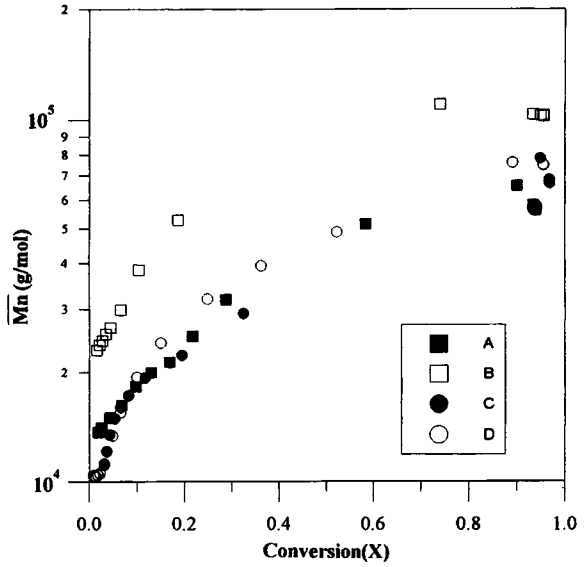

Figure 6 Accumulated number average molecular weight of polymer versus conversion.

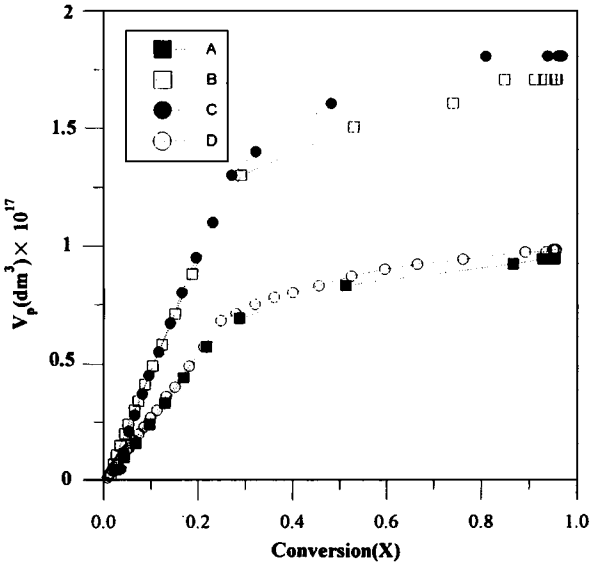

Figure 8 Volume of a swollen polymer particle versus conversion.

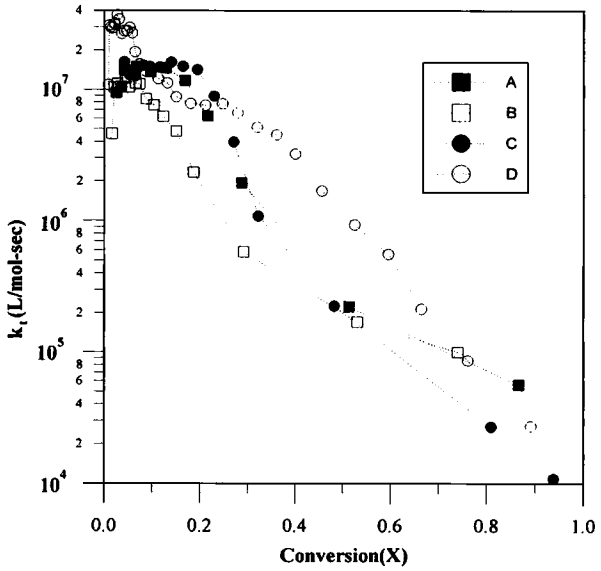

Figure 9 Termination rate constant versus conversion.

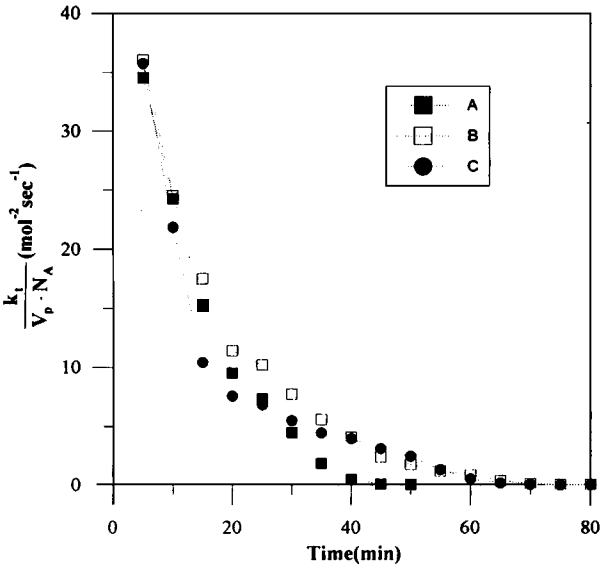

Figure 10 $\frac{k_t}{V_p \cdot N_A}$ versus time.

might be that the higher agitation speed increased the number of polymer particles, so $\bar{n}$ was lower.

Number Average Molecular Weight of Polymers

The accumulated number average molecular weight of polymers ($\overline{Mn}$) was determined by gel permeation chromatography (GPC)-analysis (Fig. 6).By substituting the GPC result into eq. (21), the instantaneous number average molecular weight ($\overline{Mn}_{\text{inst}}$) could be calculated by numerical integration. The result was shown in Figure 7. During the reaction, $\overline{Mn}_{\text{inst}}$ increased, first, with the increase of conversion because the polymerization was dominated by propagation. As the conversion became high, the viscosity in polymer particles increased rapidly and limited the mobility of longer polymer chains, so the chance for the growth of short chains increased. This was the reason why the value of $\overline{Mn}_{\text{inst}}$ decreased rapidly in the end. If the reaction temperature, initiator concentration, or agitation speed increased, it lessened the initial value of $\overline{Mn}_{\text{inst}}$.

Volume of a Swollen Polymer Particle (V_p)

The definition of $[M]_p$ was as follows:

$$[M]_p = \frac{V_{\text{monomer}} \cdot \rho_m}{M_0 \cdot (V_{\text{polymer}} + V_{\text{monomer}})} \tag{23}$$

Table III Parameters Used in the Simulation

	T(K)		
	333	343	Reference
k_d (l/s)	3.16×10^{-6}	9.23×10^{-6}	22
f	0.9	0.9	22
k_p (L/mol-s)	543	668	20
k_t (L/mol-s)	2.43×10^{7}	2.69×10^{7}	20
kD (l/s)	1.08×10^{-6}	1.08×10^{-6}	20
R_{jcr} (mol/L-H_2O)	2.74×10^{-9}	2.74×10^{-9}	18
R_{tot} (mol/L-H_2O)	3.05×10^{-8}	4.97×10^{-8}	23
$\overline{k_a}$ (L/mol-s)	2.83×10^{6}	2.83×10^{6}	23
k_{f_0} (L/mol-s)	1.45×10^{10}	1.81×10^{10}	23
t_0 (s)	20	20	23

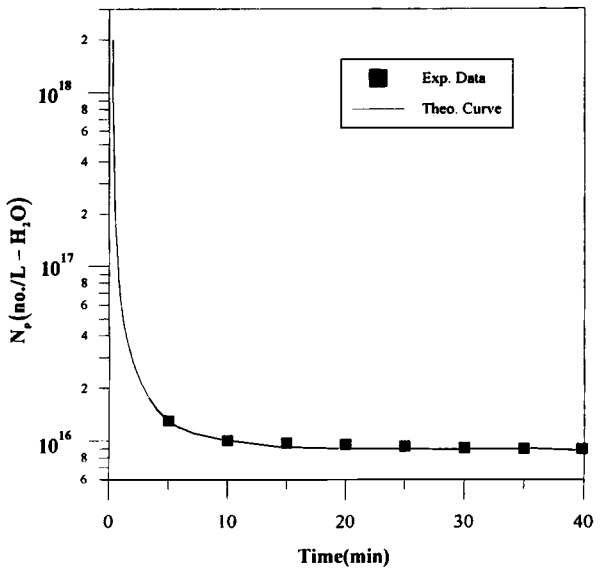

Figure 11 Concentration of polymer particles versus time for experimental condition A: theoretical calculation (– – –) and experimental result (☑).

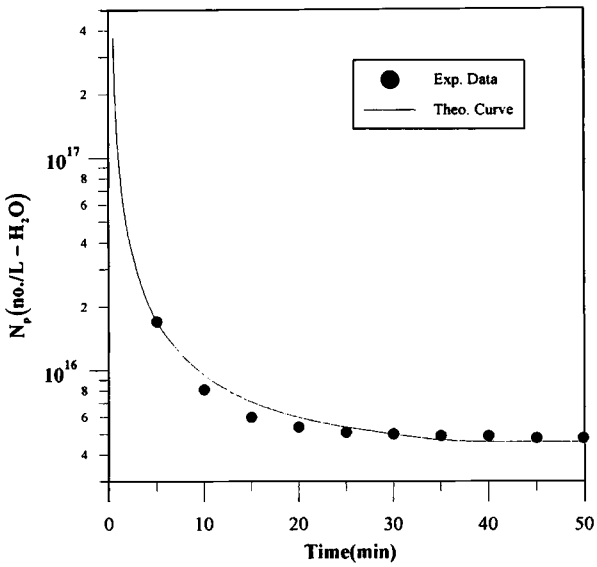

Figure 13 Concentration of polymer particles versus time for experimental condition C: theoretical calculation (– – –) and experimental result (●).

where V_{polymer} was the volume of polymer in a polymer particle, V_{monomer} was that of the monomer, ρ_m expressed the monomer density, and M_0 represented the molecular weight of monomer. Equation (23) could be rearranged as

$$V_{\text{monomer}} = \frac{[M_p] \cdot V_{\text{polymer}}}{\frac{\rho_m}{M_0} - [M]_p} \tag{24}$$

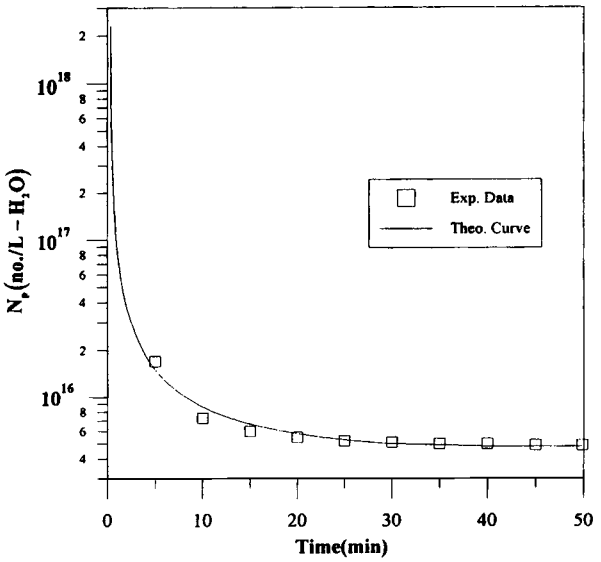

Figure 12 Concentration of polymer particles versus time for experimental condition B: theoretical calculation (– – –) and experimental result (□).

Using TEM measurement, the number average diameter of dry polymer particles ($\bar{D}$) was obtained. It was the diameter of one particle which contained no monomer. Substituting eq. (24) into (23), V_p was expressed as

$$V_p = V_{\text{polymer}} + V_{\text{monomer}} = \left(1 + \frac{[M]_p}{\frac{\rho_m}{M_0} - [M]_p}\right) \cdot V_{\text{polymer}} \tag{25}$$

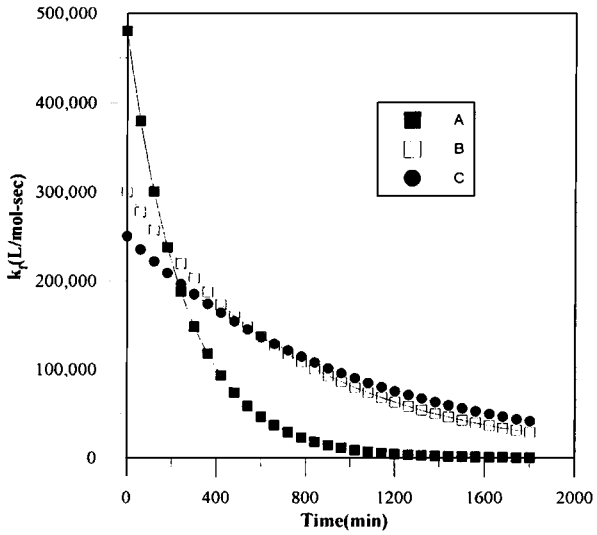

Figure 14 Coagulation rate constant versus time at different experimental conditions.

Table IV Optimal Values of Parameters *a* and *b* in Eq. (18)

Symbol	*a*	*b*
A	1.84×10^{-16}	4.99×10^{-13}
B	5.98×10^{-17}	4.96×10^{-13}
C	4.69×10^{-17}	5.04×10^{-13}

According to the definition described above, V_{polymer} was expressed as

$$V_{\text{polymer}} = \frac{4}{3} \cdot \pi \cdot \left(\frac{\bar{D}}{2}\right)^3 \quad (26)$$

Under different experimental conditions, the variation of V_p during the reaction could be calculated using eqs. (25) and (26). This was shown in Figure 8. V_p increased rapidly in the range of conversion below 0.25, then gradually leveled off as the conversion exceeded 0.25. The reason might be that the monomer droplets disappeared when the conversion was above 0.25, so there was no more abundant monomer available to maintain the growth of polymer particles. According to Figure 8, higher reaction temperatures or agitation speeds lessened the growth rate of V_p and resulted in a smaller value of V_p at final.

Termination Rate Constant (k_t)

Combining with the values of R_p, $\bar{n}$, V_p, and $\overline{Mn}_{\text{inst}}$, as shown in Figures 1–8, the termination rate constant (k_t) could be calculated from eq. (21). The result was described in Figure 9. The initial value of k_t (i.e., k_{t0}) was about 2×10^7 (L/mol-sec). This coincided with the value reported in other references.[21] When the conversion became higher, the value of k_t decreased rapidly because of the gel effect. If a higher temperature was chosen, it decreased the viscosity in polymer particles, which lessened the gel effect, so the value of k_t dropped slower. As the initiator concentration increased, the polymer chain became shorter in length. This resulted in a reduction in gel effect too. For the same reason, a higher agitation speed decreased the molecular weight of polymers, so the gel effect became less significant, and k_t decreased slower by increasing the conversion.

Simulation of Concentration of Polymer Particles

The parameters used in the simulation of concentration of polymer particles were all listed in Table III. According to the mechanism of homogeneous nucleation mentioned in the theoretical part of this article, the concentration of polymer particles could be simulated if eqs. (12)–(15) were solved by numerical calculation simultaneously. The variation of the term $\frac{k_t}{V_p \cdot N_A}$ with reaction time under different experimental conditions was shown in Figure 10. If the fourth-order polynomial was chosen to fit these curves, they could be expressed as followed, respectively. For experimental condition A,

$$\frac{k_t}{V_p \cdot N_A}(t) = 1.56 \times 10^{-5}t^4 - 2.21 \times 10^{-3}t^3 + 1.28 \times 10^{-1}t^2 - 3.84t + 51.07 \quad (27)$$

For experimental condition B,

$$\frac{k_t}{V_p \cdot N_A}(t) = 5.17 \times 10^{-6}t^4 - 1.09 \times 10^{-3}t^3 + 8.54 \times 10^{-2}t^2 - 3.14t + 49.06 \quad (28)$$

For experimental condition C,

$$\frac{k_t}{V_p \cdot N_A}(t) = 1.10 \times 10^{-5}t^4 - 2.18 \times 10^{-3}t^3 + 1.53 \times 10^{-1}t^2 - 4.59t + 54.35 \quad (29)$$

All the polynomial equations [eqs. (27)–(29)] were substituted into the theoretical calculation. In eq. (18), parameters a and b were adjustable variables. Other parameters needed in calculation were given in Table II. If the Runge-Kutta fourth-order method was selected, the concentration profile of polymer particles at different conditions could be simulated. They were all depicted in Figures 11–13. They revealed that the theoretically simulated values conformed with the experimental data very well. The variation of the rate constant of coagulation k_f versus reaction time was depicted in Figure 14. The optimal values of a and b at different experimental conditions were listed in Table IV. According to the results of simulation, the coagulation effect was serious at the beginning of the reaction, then diminished gradually. This coincided with the conclusion of Fitch and Tsai.[7] From Figure 14, we found different coagulation effects at different reaction temperatures, but the change of initiator concentration didn't significantly affect the coagulation rate constant.

CONCLUSION

In this article, a homogeneous nucleation model was used to simulate the concentration of polymer particles under different experimental conditions for soapless emulsion polymerization of MMA. The simulation conformed well with empirical data. From the calculation, we could also simulate the coagulation rate constant k_f. If a higher reaction temperature was chosen, the curve of k_f versus time declined more rapidly, but changes in initiator concentration had no apparent effect on the coagulation behavior. The average number of radicals per polymer particle $\bar{n}$ was about 0.5 when the conversion was below 15%; it increased rapidly as the gel effect became more serious. An increase in reaction temperature, initiation concentration, or agitation speed could lessen the gel effect to some extent, which reflected in the variation of termination rate constant k_t during the reaction.

The researchers greatly appreciate the financial support given by the National Science Council of the Republic of China with the grant NSC 82-0405-E002-174.

REFERENCES

1. B. M. E. Van der Hoff, *Advances in Chemistry Series,* Vol. 34, Am. Chem. Soc., Washington, D.C., 1967, p. 6.
2. A. R. Goodall, M. C. Wilkison, and M. C. Hearn, *J. Polym. Sci., Polym. Chem. Ed.,* **15,** 2193 (1977).
3. R. A. Cox, M. C. Wilkinson, A. R. Goodall, and J. M. Creasey, *J. Polym. Sci., Polym. Chem. Ed.,* **15,** 2311 (1977).
4. C. Y. Chen and I. Piirma, *J. Polym. Sci., Polym. Chem. Ed.,* **18,** 1979 (1980).
5. J. W. Vanderhoff, *J. Polym. Sci., Polym. Symp.,* **72,** 161 (1985).
6. W. J. Priest, *J. Phys. Chem.,* **56,** 1077 (1952).
7. R. M. Fitch and C. H. Tsai, *Polymer Colloids,* Plenum, New York, 1971, p. 73.
8. R. M. Fitch, *Brit. Polym. J.,* **5,** 467 (1973).
9. F. K. Hansen and J. Ugelstad, *J. Polym. Sci., Polym. Chem. Ed.,* **16,** 1953 (1978).
10. F. K. Hansen and J. Ugelstad, *J. Polym. Sci., Polym. Chem. Ed.,* **17,** 3033 (1979).
11. F. K. Hansen and J. Ugelstad, *J. Polym. Sci., Polym. Chem. Ed.,* **17,** 3047 (1979).
12. F. K. Hansen and J. Ugelstad, *Rub. Chem. Tech.,* **49,** 536 (1976).
13. F. K. Hansen and J. Ugelstad, *Emulsion Polymerization,* Academic Press, New York, 1982, Chap. 1.
14. Y. C. Chen, C. F. Lee, and W. Y. Chiu, *J. Appl. Polym. Sci.,* to appear.
15. R. W. Garrett, D. J. T. Hill, J. H. O'Donnell, P. J. Pomery, and C. L. Winzor, *Polym. Bull.,* **22,** 611 (1989).
16. S. Zhu, Y. Tian, and A. E. Hamielec, *Macromolecules,* **23,** 1144 (1990).
17. H. R. Chang, H. Y. Parker, and D. G. Westmoreland, *Macromolecules,* **25,** 5557 (1992).
18. Z. Song and G. W. Poehlein, *J. Colloid Interf. Sci.,* **128,** 486 (1989).
19. W. V. Smith and R. H. Ewart, *J. Chem. Phys.,* **16,** 592 (1948).
20. M. Arai, K. Arai, and S. Saito, *J. Polym. Sci., Polym. Chem. Ed.,* **17,** 3655 (1979).
21. G. R. Cutting, *Macromolecules,* **26,** 951 (1993).
22. Z. Song and G. W. Poehlein, *J. Polym. Sci., Polym. Chem. Ed.,* **28,** 2359 (1990).
23. Y. C. Chen, MS Thesis, Institute of Materials Science & Engineering, National Taiwan University, Taiwan, 1993.

Received December 15, 1995
Accepted March 30, 1996